TUNGSTEN NUCLEAR ANOMALIES IN PLANETESIMAL CORES

Liping Qin,[1,2] Nicolas Dauphas,[1] Meenakshi Wadhwa,[3] Agnès Markowski,[4] Roberto Gallino,[5]
Philip E. Janney,[3] and Claudia Bouman[6]

ABSTRACT

Use of the extinct ^{182}Hf-^{182}W chronometer to constrain the timing of planetary accretion and differentiation rests on the assumption that the solar nebula had homogeneous tungsten isotopic composition. Here, we report deficiencies of $\sim$0.1 part in 10,000 in the abundance of ^{184}W in group IVB iron meteorites relative to the silicate Earth. These are most likely due to incomplete mixing at the planetesimal scale (2–4 km radius bodies) of the products of slow (s-) and rapid (r-) neutron-capture nucleosynthesis in the solar nebula. The correction that must be applied to the ^{182}Hf-^{182}W model age of core formation in IVB irons due to the presence of these nuclear anomalies is $\sim$0.5 Myr.

Subject headings: minor planets, asteroids — nuclear reactions, nucleosynthesis, abundances —
solar system: formation — stars: abundances

Online material: color figures

1. INTRODUCTION

Planets and planetesimals are thought to have formed from the accretion of material with a bulk composition similar to chondritic meteorites. Subsequent melting induced differentiation (i.e., segregation of metal and silicate), the timing of which can be determined by measuring the abundance of ^{182}W, a decay product of short-lived ^{182}Hf ($t_{1/2} = 8.9 \pm 0.09$ Myr; Vockenhuber et al. 2004). Using this extinct radioactivity, it is possible to establish the accretion timescales of Earth and Mars, date the Moon-forming impact, and date magmatic differentiation events in meteorite parent bodies (e.g., Quitté et al. 2000; Yin et al. 2002; Kleine et al. 2002; Schoenberg et al. 2002; Lee et al. 2002; Foley et al. 2005; Markowski et al. 2006a).

However, use of the extinct ^{182}Hf-^{182}W chronometer to date these early solar system events rests on the assumption that the solar system had homogenous W isotopic composition. Planetary-scale isotopic anomalies have been documented for O (Clayton 1993), Cr (Trinquier et al. 2007), Mo (Dauphas et al. 2002, 2004), Ru (Chen et al. 2003), Ba (Hidaka et al. 2003), Sm, and Nd (Andreasen & Sharma 2006; Carlson et al. 2007). For heavy elements, these variations may reflect incomplete mixing of products of stellar nucleosynthesis (s-, r-, and p-processes) in the solar nebula. Similar anomalies, albeit of much larger magnitudes, were also measured in single presolar grains that formed in stellar outflows before formation of the Sun (Zinner et al. 1991; Nicolussi et al. 1997, 1998a, 1998b, 1998c; Savina et al. 2003, 2004; Barzyk et al. 2006; Terada et al. 2006). The presence of these anomalies calls into question the assumption that the early solar system was thoroughly homogenized, which can undermine the use of several short-lived radiochronometers, including ^{182}Hf.

Tungsten possesses five stable isotopes, ^{180}W, ^{182}W, ^{183}W, ^{184}W, and ^{186}W (0.1198, 26.4985, 14.3136, 30.6422, and 28.4259 atomic percent, respectively; Völkening et al. 1991). Excluding ^{180}W, which has too low of an abundance to be measured with sufficient precision, and ^{186}W and ^{183}W, which are used for correcting the measurements for instrumental mass fractionation in both this study and previous work (e.g., Yin et al. 2002; Quitté et al. 2000; Markowski et al. 2006a), the only other abundant W isotope besides ^{182}W remaining to quantify the degree of mixing of nucleosynthetic sources in the solar nebula is ^{184}W. In order to document the degree of homogenization of the solar nebula for the products of stellar nucleosynthesis, we have measured the W isotopic compositions of some magmatic iron meteorites that are thought to be remnants of planetesimal cores. The ultimate goals are to refine the s-process path in the W mass region and correct for any nucleosynthetic anomalies that could affect ^{182}Hf-^{182}W chronology in meteorites.

A brief overview of the methods used for separating and analyzing W is given in § 2. The results of iron meteorite measurements and a critical evaluation of possible analytical artifacts are presented in § 3. Possible causes for the presence of W isotopic anomalies in iron meteorites (Galactic cosmic-ray irradiation and nucleosynthetic heritage), as well as consequences for ^{182}Hf-^{182}W chronology, are discussed in §§ 4 and 5.

2. MATERIALS AND METHODS

We measured the W isotopic compositions of four IIAB iron meteorites (Cedartown, Smithsonian, Sierra Gorda, and El Burro), six IVBs (Tlacotepec, Tawallah Valley, Santa Clara, Hoba, Cape of Good Hope, and Skookum), and one ungrouped iron (Deep Springs). Tungsten was separated from matrix and isobar elements using ion exchange chromatography, and its isotopic composition was analyzed by multicollector inductively coupled plasma mass spectrometry (MC-ICPMS; for details see Foley et al. 2005; Qin et al. 2007).

The iron meteorite samples weighing 1–3 g were first leached with 11 M HCl ($\sim$20% mass loss) in order to remove any surface-sited terrestrial contamination. The cleaned pieces were then dissolved in aqua regia to ensure thorough dissolution of the sample

[1] Origins Laboratory, Department of the Geophysical Sciences and Enrico Fermi Institute, University of Chicago, 5734 South Ellis Avenue, Chicago, IL 60637; and Department of Geology, The Field Museum, 1400 South Lake Shore Drive, Chicago, IL 60605; lqin@ciw.edu.
[2] Current address: Department of Terrestrial Magnetism, Carnegie Institution of Washington, 5241 Broad Branch Road, NW, Washington, DC 20015.
[3] Department of Geology, The Field Museum, 1400 South Lake Shore Drive, Chicago, IL 60605; current address: Center for Meteorite Studies, School of Earth and Space Exploration, Arizona State University, Box 871404, Tempe, AZ 85287.
[4] Institute for Isotope Geology and Mineral Resources, Department of Earth Sciences, ETH Zentrum, NW C68.1, Clausiusstrasse 25, CH-8092 Zürich, Switzerland.
[5] Dipartimento di Fisica Generale dell'Universitá di Torino, Turin, Italy.
[6] Thermo Fisher Scientific, Hanna-Kunath-Strasse 11, 28199 Bremen, Germany.

and oxidation of FeO and Fe^{2+} to Fe^{3+}. The samples were dried down and redissolved in a minimum amount of $\sim$11 M HCl. The solutions were diluted with Milli-Q water to 110 ml (the sample must be split into two parts if more than 1.7 g is dissolved to get a final HCl molarity of less than 0.5 M). Hydrogen peroxide was added to a final concentration of 0.3% in order to stabilize W in solution.

Chemical separation of W from matrix and interfering elements was achieved through a two-stage column chemistry. The sample solution was first loaded on a 150 mL Savillex Teflon column (inside diameter [I.D.] = 4 cm) filled with 60 mL of (wet) Bio-Rad AG50-X8 200–400 mesh hydrogen-form resin, which was pre-equilibrated with 250 mL of 0.2 M HCl$-$0.3% H_2O_2. The eluate was collected and another 140 mL of 0.2 M HCl$-$0.3% H_2O_2 was added to the column to elute any remaining W. After this column, >99% of the matrix elements, mainly Fe and Ni, were removed. The eluate was then evaporated to incipient dryness. A few drops of $HClO_4$ were added, and the solution was evaporated at $\sim$200°C to get rid of carbon compounds from the sample and resin. Further purification was achieved through a series of anion-exchange columns in HCl-HF medium, following the procedure of C. N. Foley (2005, personal communication) from Münker et al. (2001) and Kleine et al. (2004). A precleaned Savillex Teflon microcolumn (I.D. = 6.4 mm) was filled with 2 mL (wet) AG1-X8 200–400 mesh chlorine-form resin. The resin was cleaned and conditioned with 10 mL of 6 M $HNO_3$$-$0.2 M HF 1%$-$$H_2O_2$, 2 mL of Milli-Q H_2O, 10 mL of 7 M HCl$-$1 M HF, and 10 mL of 0.5 M HCl$-$0.5 M HF. The sample solution (1 mL) in 1 M HCl$-$0.5 M HF was loaded on the column, and 8 mL of 0.5 M HCl$-$0.5 M HF, 4 mL of 0.5 mM HCl$-$0.5 mM HF, 13 mL of 9 M HCl$-$0.01 M HF, 1 mL of 9 M HCl$-$1 M HF were added to elute remaining matrix elements and interfering elements. Tungsten was collected in 11 mL of 7 M HCl$-$1 M HF. One drop of $HClO_4$ was then added to the W eluate to prevent complete drying during evaporation and promote loss of Os and organic compounds. The anion-exchange chemistry was repeated for a total of three times, changing the resin each time. A number of cycles (typically three) of drying down the sample in $HClO_4$ and taking it back in solution in a drop of the same acid were performed at the end of the last anion-exchange sequence.

The isotopic compositions of purified W solutions in 0.5 M $HNO_3$$-$0.01 M HF were analyzed using a Micromass Isoprobe MC-ICPMS instrument at the Isotope Geochemistry Laboratory of the Field Museum. Ion intensities of ^{179}Hf, ^{180}Hf $+$ ^{180}Ta $+$ ^{180}W, ^{181}Ta, ^{182}W, ^{183}W, ^{184}W $+$ ^{184}Os, ^{186}W $+$ ^{186}Os, and ^{188}Os were measured on Faraday collectors. Measuring ^{179}Hf, ^{181}Ta, and ^{188}Os allowed us to monitor and correct for isobaric interferences from Hf, Ta, and Os. The sample was run at 30–80 parts per billion (ng/g), corresponding to ion intensities in the range $(3–8) \times 10^{-11}$ A (measured with 10^{11} Ω resistors). Most of the measurements were conducted under "hard extraction" mode (in which a negative voltage is applied to the collimator cone). The samples were measured in a sequence of 20 cycles, with each cycle integrating ion intensities for 15 s. A NIST 3163 W solution was used as the W isotope standard. The W concentration of the standard was matched with that of the sample to within 3%. Sample measurements were bracketed by standard measurements to correct for instrument response drift with time. Natural and instrumental mass fractionations were corrected using the exponential law (Maréchal et al. 1999), in which the isotope ratios (^{182}W/^{183}W and ^{184}W/^{183}W) were normalized to a fixed ^{186}W/^{183}W ratio of 1.98594 (Völkening et al. 1991). The ε-value (the relative deviation of internally normalized isotope ratio from the standard $\times 10^4$) of the sample was calculated relative to the average of the adjacent standards. A total of 13–20 repeats were obtained for each sample and were used to compute averages and 95% confidence intervals as

$$\varepsilon = \frac{1}{n}\sum_{k=1}^{n} \varepsilon_k \pm \sqrt{\frac{1}{n-1}\sum_{k=1}^{n}(\varepsilon_k - \varepsilon)^2} \frac{t_{0.95,n-1}}{\sqrt{n}}$$

where $t_{0.95,n-1}$ is Student's t-value corresponding to a two-sided 95% confidence interval for $n-1$ degrees of freedom.

3. W ISOTOPIC ANOMALIES

The results of W isotopic composition are compiled in Table 1. For the purpose of interlaboratory comparison, some of the samples were also measured on Neptune and Nu plasma MC-ICPMS.

The ε^{182}W values obtained for IIAB and IVB iron meteorites agree with a recent study (Markowski et al. 2006a), and the chronological implications will be discussed in a separate contribution. For ε^{184}W values, no variation outside analytical uncertainties is observed within each group (Fig. 1). IIAB meteorites show no deviation in ε^{184}W relative to the NIST 3163 terrestrial W standard, within error (0.01 $\pm$ 0.03). The IVBs and the ungrouped iron Deep Springs show deficiencies in ε^{184}W of -0.08 ± 0.01 and -0.15 ± 0.02, respectively.

The ε^{184}W deficiencies measured in Deep Springs and Tlacotepec are small, and it is the first time that such effects are reported in iron meteorites. For those reasons, we evaluated a number of analytical artifacts that may have affected W isotope analyses, particularly ε^{184}W.

1. We found that mismatch in the W concentration between standards and samples can affect the accuracy of the ε^{184}W measurements, if the difference is larger than 3% (Qin et al. 2007). Care was taken to match the W concentration of the sample with that of the standard within 3% for all reported measurements.

2. Peak scans of selected W solutions in the atomic mass range 40–220 were compared with those of blank solutions. Figure 2 shows such a scan for Tlacotepec. The final purified W sample solution is very clean. No peaks indicating the presence of matrix and interfering elements were observed over the entire mass range. In addition, no molecular interferences are observed around the W mass region. Osmium, a major isobar of W was monitored and corrected in every analysis and was always present at a very low abundance, with ^{188}Os/^{186}W intensity ratios of $\sim 10^{-5}$, corresponding to a negligible correction of $<0.01\varepsilon$ on ε^{184}W. A potential isobar on ^{184}W$^+$, ^{92}Mo^{92}Mo$^+$, was checked for a few sample solutions through monitoring ^{92}Mo$^+$ peak intensities. The intensity of ^{92}Mo$^+$ is always very low, and the maximum ^{92}Mo/^{184}W intensity ratio is $<10^{-3}$. Using a 1 part per million (μg/g) pure Mo solution, we did a peak scan in the mass range 184–200 to search for the potential presence of diatomic molecules. The Mo_2^+/Mo^+ ratio is estimated to be $<2 \times 10^{-5}$. Assuming that isotopes are associated in diatomic molecules in a random manner, ^{92}Mo^{92}Mo$^+$ only represents 2.2% of Mo_2^+. Another isobar, ^{92}Mo^{94}Mo$^+$ on ^{186}W$^+$, only represents 2.7% of Mo_2^+. Based on these numbers, the computed shift on ε^{184}W due to the presence of Mo is negligible. In addition, we do not see any correlation of ε^{184}W with the number of anion-exchange columns through which the samples were processed, while the Mo/W ratio in the solution is expected to decrease with increasing column number (Fig. 3). IIAB meteorites also have Mo/W ratios similar to IVB meteorites (Petaev & Jacobsen 2004), but do not show ε^{184}W deficiencies. A W standard was doped with Mo (Mo:W = $\sim$1:10), and the measured

TABLE 1
W Isotopic Values for Iron Meteorites from This Study

Sample	Specimen	$\varepsilon^{182}W$	$\varepsilon^{184}W$	N
IIAB				
Cedartown 1a................................	ME 2373	−3.36 ± 0.05	0.01 ± 0.04	17
Cedartown 1b[a]................................	ME 2373	−3.33 ± 0.18	0.04 ± 0.10	5
Cedartown 2[b]................................	ME 2373	−3.58 ± 0.10	0.00 ± 0.11	9
Mean		−3.39 ± 0.04	0.01 ± 0.03	
Smithsonian................................	ME 2383	−3.42 ± 0.05	0.02 ± 0.06	15
Sierra Gorda................................	USNM 1307	−3.47 ± 0.08	−0.02 ± 0.07	13
El Burro	ME 2848	−3.52 ± 0.11	−0.01 ± 0.09	16
Group Mean................................			0.01 ± 0.03	
IVB				
Tawallah Valley 1	ME 2705	−3.53 ± 0.06	−0.10 ± 0.02	18
Tawallah Valley 2	ME 2705	−3.53 ± 0.05	−0.07 ± 0.05	16
Mean		−3.53 ± 0.04	−0.10 ± 0.02	
Santa Clara................................	ME 2859	−3.62 ± 0.06	−0.06 ± 0.03	16
Hoba................................	ME 2477	−3.43 ± 0.08	−0.07 ± 0.05	16
Cape of Good Hope................................	ME 424	−3.71 ± 0.06	−0.12 ± 0.04	15
Skookum................................	ME 1963	−3.55 ± 0.1	−0.11 ± 0.05	16
Tlacotepec 1a	ASU-113ax	−4.02 ± 0.07	−0.10 ± 0.06	17
Tlacotepec 1b[a]	ASU-113ax	−3.95 ± 0.04	−0.05 ± 0.02	7
Tlacotepec 2	ASU-113ax	−4.04 ± 0.09	−0.09 ± 0.04	14
Tlacotepec 3	ASU-113ax	−4.14 ± 0.07	−0.06 ± 0.05	17
Tlacotepec 4	ASU-113ax	−4.22 ± 0.08	−0.07 ± 0.06	13
Tlacotepec 5	ASU-113ax	−4.22 ± 0.07	−0.11 ± 0.03	15
Tlacotepec 6	ASU-113ax	−4.25 ± 0.05	−0.09 ± 0.02	16
Tlacotepec 7	ASU-113ax	−4.11 ± 0.16	−0.05 ± 0.08	11
Tlacotepec 8a	ASU-113ax	−4.20 ± 0.07	−0.09 ± 0.05	17
Tlacotepec 8b	ASU-113ax	−4.13 ± 0.06	−0.05 ± 0.04	15
Tlacotepec 9	ME 2159 5	−4.01 ± 0.05	−0.15 ± 0.04	25
Mean		−4.10 ± 0.02	−0.08 ± 0.01	
Group Mean................................			−0.08 ± 0.01	
Ungrouped				
Deep Springs 1a................................	ME 453	−3.80 ± 0.06	−0.19 ± 0.05	16
Deep Springs 1b[a]................................	ME 453	−3.75 ± 0.06	−0.14 ± 0.03	2
Deep Springs 2	ME 453	−3.78 ± 0.05	−0.15 ± 0.06	13
Deep Springs 3	ME 453	−3.77 ± 0.10	−0.26 ± 0.09	12
Deep Springs 4[b]................................	ME 453	−3.74 ± 0.11	−0.12 ± 0.05	10
Mean		−3.77 ± 0.02	−0.15 ± 0.02	
NIST 3163 W		−0.03 ± 0.07	−0.01 ± 0.05	12
NIST 3163 W + Tlacotepec matrix		0.07 ± 0.11	−0.01 ± 0.06	11

Notes.—The $\varepsilon^{182}W$ and $\varepsilon^{184}W$ are the relative deviation from NIST 3163 W standard; $\varepsilon^{i}W = [({}^{i}W/{}^{183}W)_{sample}/({}^{i}W/{}^{183}W)_{std} - 1] \times 10^{4}$; N represents number of repeats. Sample arabic numeral suffixes represent separate dissolutions of different pieces of meteorite samples. Lower case letter suffixes represent different aliquots of the same dissolution. All the analyses were obtained by Isoprobe MC-ICPMS, unless otherwise indicated.
[a] Analyses by Neptune MC-ICPMS (Thermo Fisher Scientific, Bremen).
[b] Analyses by Nu-plasma MC-ICPMS (ETH, Zürich). A different chemical protocol from that discussed in the text was used. The details can be found in Markowski et al. (2006a).

$\varepsilon^{184}W$ and $\varepsilon^{182}W$ values are normal within uncertainties (0.03 ± 0.05 and 0.04 ± 0.08, respectively). Finally, ${}^{92}Mo{}^{92}Mo^{+}$ interference is expected to create excess in $\varepsilon^{184}W$, not deficiencies as is observed.

3. A pure NIST 3163 W standard was processed through the W separation procedure. An aliquot of the NIST W standard was also mixed with the matrix elements (Fe, Ni, and Co, without elements that follow W during the chemistry) of Tlacotepec recovered from the chemistry and was processed through the W separation procedure. The measured $\varepsilon^{184}W$ values of these two solutions (Table 1; Fig. 1) are identical to that of the unprocessed, pure NIST 3163 W standard, indicating that there are no ana-

lytical artifacts related to the sample matrix or the W separation procedure.

4. Multiple analyses of Tlacotepec were performed to check the reproducibility of the results by Isoprobe MC-ICPMS when changing either the number of cation/anion exchange columns used for chemical separation or the ion extraction mode of the instrument. The $\varepsilon^{184}W$ values for these multiple Tlacotepec analyses (Isoprobe only) are shown in Figure 3. Changing the number of cation/anion exchange columns is a useful test to evaluate the effect of residual matrix elements and isobars, since samples passed through various cation/anion column combinations are expected to contain various levels/compositions of
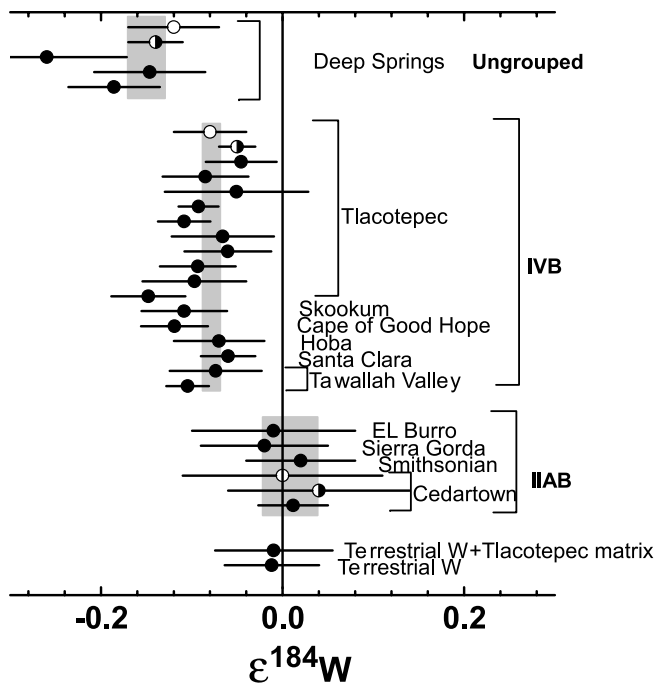
Fig. 1.—ε^{184}W values for IVB, IIAB, and Deep Springs (ungrouped) iron meteorites (Table 1). Also shown are the ε^{184}W values for pure NIST 3163 W standard as well as the NIST W standard mixed with matrix elements recovered from the elution of Tlacotepec, both of which were processed through the W separation procedure. Solid symbols, half-open, and open symbols correspond to measurements obtained by Isoprobe, Neptune, and Nu-plasma MC-ICPMS instruments, respectively. The Tlacotepec datum by Nu-plasma is from Markowski et al. (2006a). The error bars are 95% confidence intervals. The gray rectangles show the weighted averages and corresponding error bars for different iron meteorite groups.

Fig. 2.—Peak scan spectra for a Tlacotepec W solution (*top*) and a mass spectrometer blank (*bottom*).

matrix elements and isobars. Some of the measurements were conducted in "soft extraction" mode, where a small positive extraction voltage is applied to the collimator cone. This typically lowers the peak sensitivity by 50%–75% compared to "hard extraction" mode, but lowers the background intensity by 90%–99%. If molecular interferences were a problem in the measurements, changing the ion extraction mode of the instrument from "hard" to "soft" mode would significantly reduce the level of molecular interferences and could result in different ε^{184}W values. Figure 3 demonstrates a good consistency in ε^{184}W values among all the Tlacotepec measurements, regardless of changes in the analytical protocol.

5. The effect of mass fractionation was examined. Column chromatography can cause mass fractionation of W isotopes if W is not fully recovered. When searching for isotopic variations that do not depend on mass, natural and laboratory-introduced mass fractionations are usually corrected for by internal normalization to a pair of isotopes using the exponential law. However, if the fractionation does not obey the exponential law, the measured ε^{184}W could change with the mass fractionation factor of the analyzed solution. Figure 4 shows that this is not the case.

6. Interlaboratory reproducibility was tested for three samples: Cedartown, Tlacotepec, and Deep Springs. The results are shown in Figure 5. The ε^{184}W values obtained by Isoprobe are consistent with those obtained in two other laboratories (ETH in Zurich and the Thermo Fisher Scientific factory in Bremen) using different types of MC-ICPMS (Nu and Neptune) for all three samples (Fig. 5a). In the case of ETH Zurich (Nu), the whole procedure, from sample dissolution to isotopic analysis (including chemical purification) was done independently. In the case of the Thermo
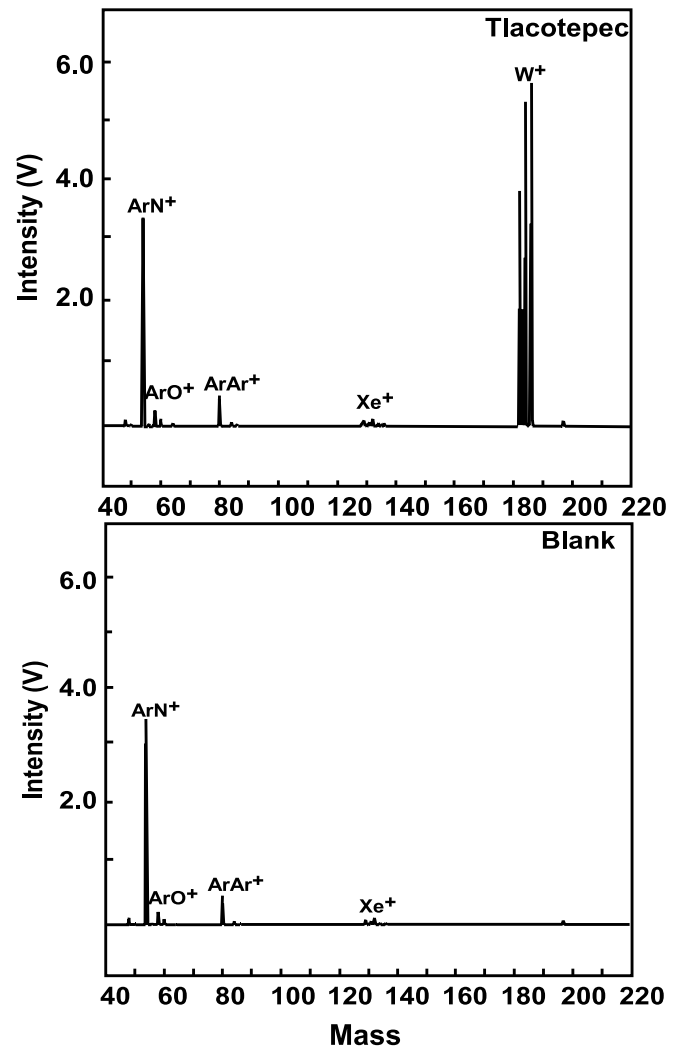
factory in Bremen (Neptune), analyses were performed on solutions that were purified in Chicago. It is doubtful that analytical artifacts would be present at the same level using different MC-ICPMS instruments and different purification protocols.

Thus, we conclude that the deficiencies of ε^{184}W in IVB iron meteorites and Deep Springs relative to the terrestrial standard and IIAB iron meteorites are real. Possible reasons for the observed ε^{184}W variations are exposure to galactic cosmic rays (GCRs) in space or heterogeneous distribution of s- and r-process isotopes in the solar nebula.

4. GALACTIC COSMIC-RAY IRRADIATION?

It has been shown both theoretically and experimentally that long-term exposure to GCR can cause negative shifts in internally normalized ε^{182}W values of iron meteorites (Masarik 1997; Leya et al. 2003; Markowski et al. 2006b). This is because GCRs can generate secondary neutrons causing W isotope shifts through neutron-capture reactions. Simulations of cosmic-ray interactions with iron meteorites indicate that for a fragment of Toluca of 3.9 m radius exposed to GCR for 600 Myr (Masarik 1997), the maximum shift in ε^{182}W (normalized by ^{186}W/^{183}W) is -0.5ε. The corresponding effect on ε^{184}W is very small ($\sim 0.03\varepsilon$), but with an uncertainty of $\sim \pm 0.2\varepsilon$ (J. Masarik 2005, personal communication). It is worthwhile to note that the absolute change in
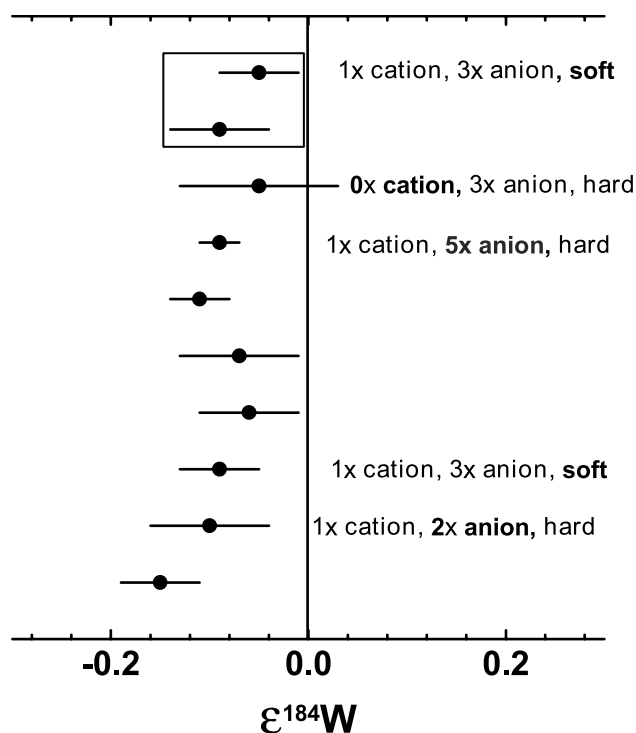
Fig. 3.—ε^{184}W values of Tlacotepec measurements on Isoprobe MC-ICPMS (Field Museum, Chicago). Details relevant to the chemical purification procedure and isotopic analysis are shown as "$m \times$ cation, $n \times$ anion, hard/soft" (m and n are the number of cation- and anion-exchange columns that the specimen was processed through, respectively; "hard/soft" represents "hard" or "soft" extraction mode of the instrument) If unlabelled as indicated above, the Tlacotepec specimens were processed and analyzed by the standard procedure described in the text (1 $\times$ cation, 3 $\times$ anion, hard). The rectangle shows that the two analyses were done on the same solution. Otherwise, different meteorite fragments were dissolved.

Fig. 4.—ε^{184}W value vs. W isotope fractionation factor in the analyzed solution for all the Tlacotepec analyses by Isoprobe. Also shown are the regression line (solid line) and its 95% confidence envelope (gray lines). The W fractionation factor in the analyzed solution was calculated relative to the bracketing standard without internal normalization, so the fractionation factor excludes instrumental mass fractionation and corresponds to the mass-dependent fractionation introduced by ion-exchange chromatography and natural processes. Because the mass fractionation by natural processes is presumably the same for all Tlacotepec pieces, this plot reflects whether or not the measured ε^{184}W value is correlated with the mass fractionation caused by ion chromatography.

^{184}W/^{183}W ratio due to GCR irradiation is significant, but because of internal normalization, the expected shift in ε^{184}W is small. Another feature of the GCR effect is that cosmogenic ε^{182}W is approximately linearly correlated with cosmogenic ε^{184}W, although the sign and value of the slope are both uncertain due to model uncertainties. The negative ε^{182}W values measured in Tlacotepec, and other meteorites (Table 1) relative to the inferred initial composition of the solar nebula (~-3.5; Yin et al. 2002; Kleine et al. 2005) is primarily caused by GCR irradiation (Masarik 1997; Leya et al. 2003; Markowski et al. 2006b), given their relatively long exposure ages (e.g., Voshage & Feldmann 1979). However, this process cannot be responsible for the ε^{184}W deficiencies measured in IVBs. Indeed, if this were the case, there should be a correlation between GCR irradiation documented by ε^{182}W and shifts in ε^{184}W (as indicated by the dashed line in Fig. 6). In addition, this correlation should pass through ε^{184}W = 0 when ε^{182}W is ~-3.5 (assuming that the original ε^{182}W value of IVBs before GCR exposure is close to the initial value inferred for the solar system, as documented for other groups of magmatic iron meteorites; e.g., Markowski et al. 2006a). This contradicts our observations that there is no correlation between ε^{182}W and ε^{184}W (slope = -0.005 ± 0.054) and that ε^{184}W is negative (-0.08 ± 0.03) when ε^{182}W = -3.5 (Fig. 6).

5. NUCLEOSYNTHETIC ANOMALIES AND IMPLICATIONS FOR ^{182}Hf-^{182}W CHRONOMETRY

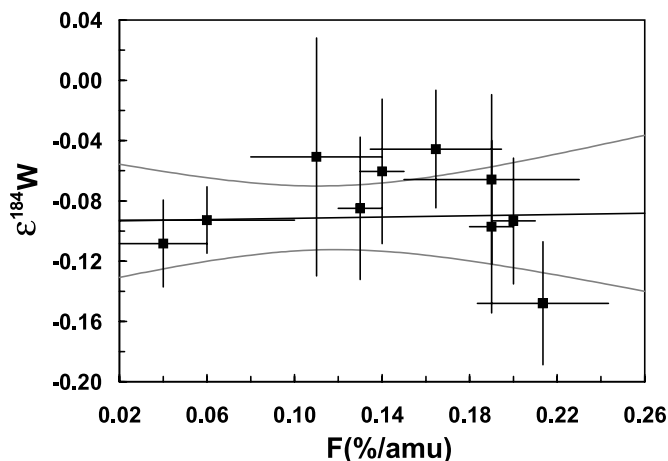The most likely interpretation for the deficiencies in ε^{184}W measured in IVBs is that these reflect inherent heterogeneous distribution of products of stellar nucleosynthesis in the solar nebula. All W isotopes except ^{180}W (mainly produced by the p-process) are synthesized by s- and r-processes in asymptotic giant branch (AGB) stars and supernovae, respectively. If different regions of the nebula received different contributions of s- or r-process isotopes, variations in the isotopic composition of W are expected. We computed s-process yields in an AGB stellar model using an updated nuclear reaction network (Bao et al. 2000). The estimated s-process abundances are similar to those reported in a previous study (Arlandini et al. 1999), except for a ^{182}W yield that was 40% higher (corresponding to a 17% increase in s-process fraction of ^{182}W) due to a 50% downward revision of the cross section of ^{182}Ta (Bao et al. 2000; Rauscher & Thielemann 2000). In Figure 7 we show the result of adding or subtracting an s-process component to or from the bulk silicate Earth (BSE) composition (solid black line). Negative ε^{184}W in IVBs can be accounted for by slight deficiencies in s- or enrichments in r-process components. This is consistent with the results of Mo (Dauphas et al. 2002, 2004) and Ru (Chen et al. 2003) isotopic studies of iron meteorites, except that s-process deficiencies in the isotopes of these two elements were also observed in IIABs. We also note that the isotopic variations for Mo and Ru are approximately 1 order of magnitude larger than those for W. Since melting and subsequent segregation of metal from silicate in iron meteorite parent bodies destroyed presolar grains (the carrier phases of nucleosynthetic anomalies), the ε^{184}W anomalies detected in IVB iron meteorites must reflect the heterogeneous distribution of s- and r-process isotopes at the scale of the IVB parent body (an asteroid of $\sim2-4$ km radius; Haack et al. 1990).

A question that needs to be addressed is whether or not nuclear anomalies have also affected ^{182}W in a way that would yield erroneous ^{182}Hf-^{182}W model ages (the time of metal-silicate differentiation in a two-stage scenario; e.g., for details see Yin et al. 2002; Kleine et al. 2002; Lee et al. 2002; Markowski et al. 2006a; Scherstén et al. 2006). Modeling of the s-process in AGB stars predicts that there should be a correlation between nonradiogenic, noncosmogenic ε^{182}W (denoted as ε^{182}W$_n$) and noncosmogenic
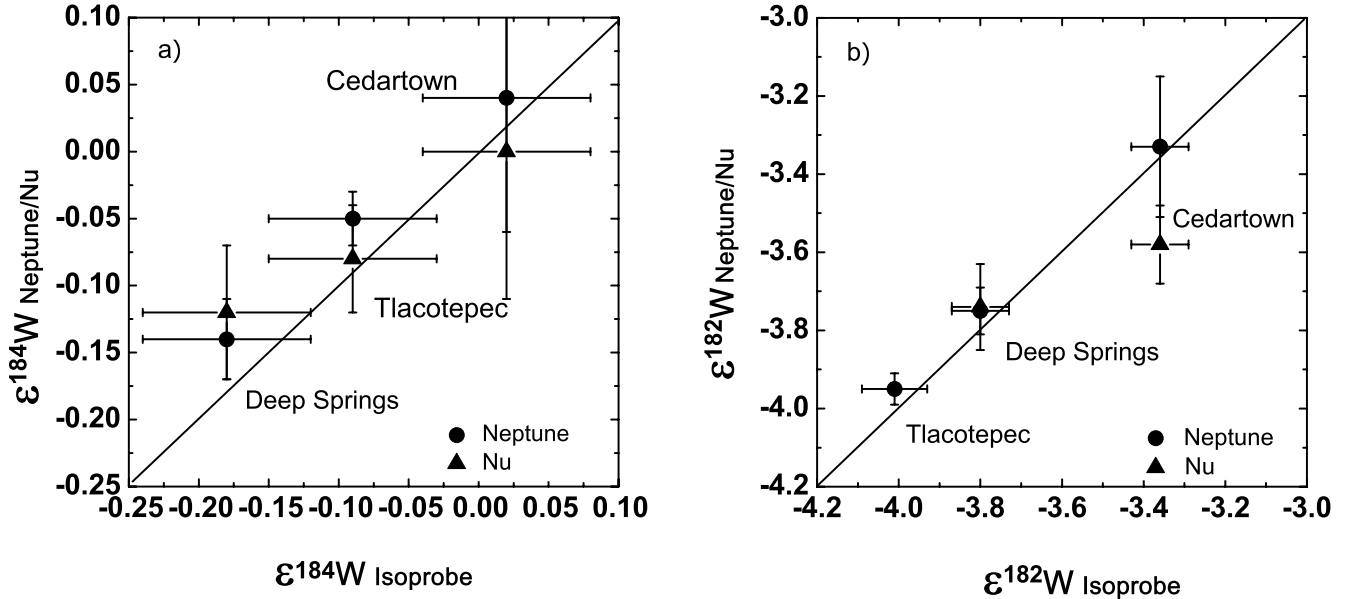
Fig. 5.—(a) ε^{184}W values and (b) ε^{182}W values for Cedartown, Deep Springs, and Tlacotepec obtained using three different types of MC-ICPMS instruments (Isoprobe, Neptune, and Nu plasma). For all three samples, the Neptune data (Thermo Fisher Scientific, Bremen) were obtained using the same solutions as those used for Isoprobe analyses. For Cedartown and Deep Springs, additional samples were obtained from areas in the specimens close to those that had been sampled previously for Isoprobe/Neptune analyses and were processed through a different separation procedure and analyzed by Nu-plasma MC-ICPMS at ETH, Zürich (see Markowski et al. 2006a for details of the analytical procedure). The Tlacotepec ε^{184}W datum by Nu-plasma is from Markowski et al. (2006a). Because of GCR-related variations in ε^{182}W in this meteorite (Markowski et al. 2006b), no direct comparison of ε^{182}W can be made for Tlacotepec between Nu plasma and the other two instruments. [See the electronic edition of the Journal for a color version of this figure.]

ε^{184}W (denoted as ε^{184}W$_n$) (both are normalized to ^{186}W/^{183}W) with a slope of 0.04 (Fig. 7). Using this value, a correction of only +0.004 needs to be made to ε^{182}W for ε^{184}W = −0.1. This is negligible compared to analytical precision and hence no correction needs to be made to model ages.

However, the slope of this correlation is still uncertain due to uncertainties in some key nuclear properties. The following factors control the s-process path and model outcomes: the neutron-capture cross sections of the stable isotopes of W and the cross sections and β^--decay rates at the branching points ^{182}Ta, ^{181}Hf, ^{182}Hf, and ^{185}W (where capture of neutrons and β-decay occur simultaneously).

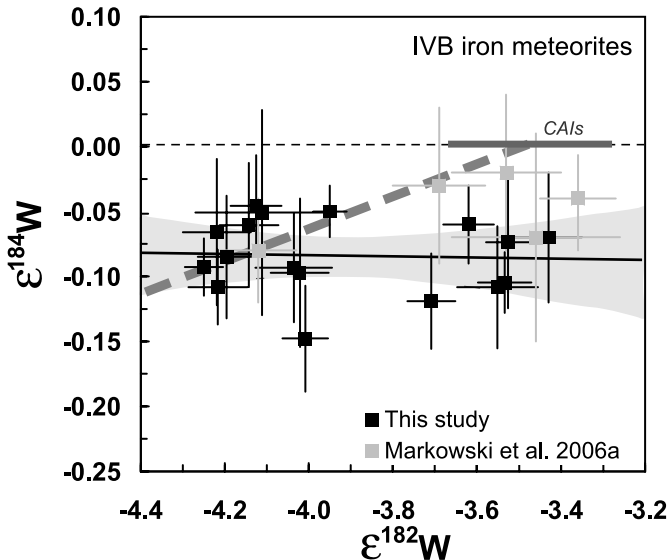

Fig. 6.—ε^{184}W vs. ε^{182}W for IVB iron meteorites from this study and Markowski et al. (2006a). The medium gray dashed line shows schematically the trend expected to result from GCR irradiation, assuming an original ε^{182}W value (before GCR exposure) for IVBs close to the initial values of CAIs (dark gray bar; Kleine et al. 2005). The straight solid line is the regression line for the measurements in this study. Also shown (in light gray) is the 95% confidence envelope of the regression line. The slope is −0.005 ± 0.054, and the value of ε^{184}W for ε^{182}W = −3.5 is −0.08ε (±0.03). This shows that GCR cannot be responsible for the deficit in ε^{184}W, because a correlation line passing through ε^{182}W = −3.5 and ε^{184}W = 0 would be expected (dashed medium gray line). [See the electronic edition of the Journal for a color version of this figure.]

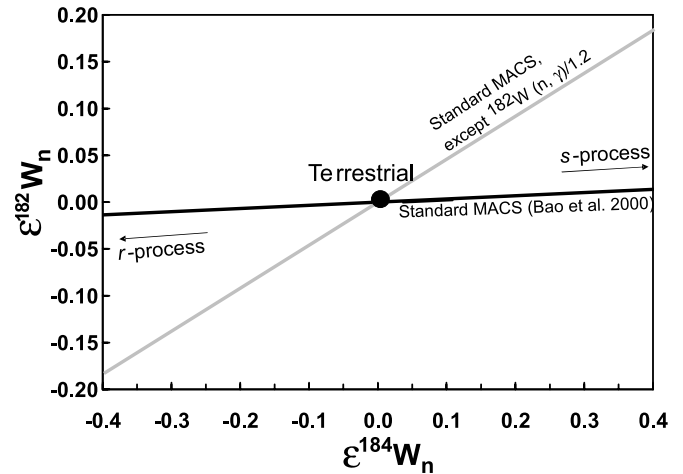Fig. 7.—Correlation between nonradiogenic, noncosmogenic ε^{182}W (ε^{182}W$_n$) and noncosmogenic ε^{184}W (ε^{184}W$_n$) for incomplete mixing of s-process W. Both values are normalized to ^{186}W/^{183}W. The slope of the correlation is given by ε^{182}W$_n$ = $(\rho_W^{182} - \rho_W^{186}\mu_W^{182})/(\rho_W^{184} - \rho_W^{186}\mu_W^{184})\varepsilon^{184}W_n$, where ρ_W^i is the s-process composition normalized to the terrestrial composition $\rho_W^i = (^iW/^{183}W)_s/(^iW/^{183}W)_\oplus - 1$, and μ_W^i is the mass difference relative to the normalizing pair (186 and 183) $\mu_W^i = (i - 183)/(186 - 183)$ (see Dauphas et al. 2004 for details). The mixing lines between terrestrial and s-process W were calculated from a nuclear reaction network in an AGB stellar model using recommended values of Maxwellian-averaged (n, γ) cross sections (MACS) from Bao et al. (2000) (black line), and using recommended values for all isotopes, except for a 20% reduction in that of ^{182}W [denoted as ^{182}W (n, γ)] (gray line).

Branching at ^{182}Ta, ^{181}Hf, and ^{182}Hf mainly affects the s-process production of ^{182}W, and branching at ^{185}W affects the s-process yield of ^{186}W. The neutron-capture cross sections of all the branching nuclides are based on theoretical calculations with relatively large uncertainties, except for ^{182}Hf, which has recently been measured (Vockenhuber et al. 2007). In addition to uncertainties in the cross sections of these isotopes, the β^--decay rate of ^{185}W increases slightly with temperature (Takahashi & Yokoi 1987), which for AGB star conditions ($10^8 < T < 3 \times 10^8$ K), leads to a -20% to $+40\%$ uncertainty in the decay rate (according to the maximum error factors affecting the β^--decay rate at given temperatures in Table 1 of Goriely 1999). The impact of these uncertainties on s-process yields was explored by running model simulations, and the results show that the combined effects of $\pm30\%$ changes in the cross sections of ^{181}Hf and ^{182}Ta, a $\pm20\%$ change in that of ^{185}W, and a -20% to $+40\%$ change in the β^--decay rate of ^{185}W result in an uncertainty of $\sim\pm0.2$ on the slope between nonradiogenic, noncosmogenic ε^{182}W$_n$ and noncosmogenic ε^{184}W$_n$. Thus, the maximum correction that must be applied to ^{182}Hf-^{182}W model ages is $\sim\pm0.2$ Myr, at a given ε^{184}W of ~-0.1.

The reported uncertainties in the recommended neutron-capture cross sections of major stable W isotopes are small (2%–3%; Bao et al. 2000) and are usually not thought to be a major source of uncertainty in nuclear reaction networks. However, some of the measurements may be inaccurate. A major concern about yields from AGB star models is the observation that the calculated r-process residue of ^{182}W (by subtracting the s-process abundance from the solar abundance of ^{182}W) shows up as a positive anomaly above the smooth r-abundance pattern, and this is unlikely to be a real feature of the r-process (Wisshak et al. 2006; Vockenhuber et al. 2007). This implies that the s-process abundance of ^{182}W may have been underestimated by the model. Changing the cross sections of ^{182}Ta and ^{181}Hf within error bars ($\pm30\%$) does not solve the problem (Vockenhuber et al. 2007). In principle, the abundance of ^{182}W resulting from the r-process could be easily reconciled with neighbor abundances if the cross section of ^{182}W itself were reduced by $\sim20\%$. The possibility that the cross section of ^{182}W may have been overestimated appears plausible, given a recent revision of $\sim30\%$ for the cross sections of ^{176}Hf and 7% for ^{180}Hf (Wisshak et al. 2006), and should be checked experimentally. A $\sim20\%$ reduction in the cross section of ^{182}W alone increases the value of the slope in Figure 7 to ~0.5. Thus, a deficit of -0.1ε in ε^{184}W would correspond to a $+0.05\varepsilon$ correction in ε^{182}W. This translates into an age correc-

tion of $+0.5$ Myr for IVB irons (time running from zero at solar system formation to 4.56 Gyr at present). We also simulated the case in which the cross sections of all even W isotopes are reduced by 20% (the cross section of the odd W isotope, ^{183}W, is twice as large as those of even W isotopes and is unlikely to have been overestimated). In this scenario, the slope changes to 0.4. A similar correction of ~0.4 Myr needs to be made to the model age.

6. CONCLUSIONS

As is attested to by variations in ε^{184}W found in IVB iron meteorites, the isotopic composition of W was not homogenized in the solar system at the scale of planetesimals up to 4 km in radius. This heterogeneity reflects incomplete mixing of the products of s- and r-neutron-capture processes. A small deficiency in s- or enrichment in r-process component in the IVB parent body can best explain the deficiencies in ε^{184}W of these meteorites. To accurately correct ε^{182}W for the presence of such anomalies and use ^{182}Hf-^{182}W as a chronometer, the yields of the s-process for W isotopes must be accurately and precisely known. This could be achieved by refining models of s-process nucleosynthesis in AGB stars as well as improving determinations of cross sections and β^--decay rates in the W mass region. The other option would be to analyze the W isotopic composition of mainstream SiC presolar grains, which are micron-sized solids found in meteorites that formed in the outflows of AGB stars and thus provide the opportunity to directly measure the isotopic pattern of the s-process.

REFERENCES

Andreasen, R., & Sharma, M. 2006, Science, 314, 806
Arlandini, C., Käppeler, F., Wisshak, K., Gallino, R., Lugaro, M., Busso, M., & Straniero, O. 1999, ApJ, 525, 886
Bao, Z. Y., Beer, H., Käppeler, F., Voss, F., & Wisshak, K. 2000, At. Data Nucl. Data Tables, 76, 70
Barzyk, J. G., Savina, M. R., Davis, A. M., Gallino, R., Pellin, M. J., Lewis, R. S., Amari, S., & Clayton, R. N. 2006, NewA Rev., 50, 587
Carlson, R. W., Boyet, M., & Horan, M. 2007, Science, 316, 1175
Chen, J. H., Papanastassiou, D. A., & Wasserburg, G. J. 2003, Lunar Planet. Sci., 34 , abs. 1789
Clayton, R. N. 1993, Annu. Rev. Earth Planet. Sci., 21, 115
Dauphas, N., Davis, A. M., Marty, B., & Reisberg, L. 2004, Earth Planet. Sci. Lett., 226, 465
Dauphas, N., Marty, B., & Reisberg, L. 2002, ApJ, 565, 640
Foley, C. N., Wadhwa, M., Borg, L. E., Janney, P. E., Hines, R., & Grove, T. L. 2005, Geochim. Cosmochim. Acta, 69, 4557
Goriely, S. 1999, A&A, 342, 881
Haack, H., Rasmussen, K. L., & Warren, P. H. 1990, J. Geophys. Res., 95, 5111
Hidaka, H., Ohta, Y., & Yoneda, S. 2003, Earth Planet. Sci. Lett., 214, 455

Kleine, T., Mezger, K., Münker, C., Palme, H., & Bishoff, A. 2004, Geochim. Cosmochim. Acta, 68, 2935
Kleine, T., Mezger, K., Palme, H., Scherer, E., & Münker, C. 2005, Geochim. Cosmochim. Acta, 69, 5805
Kleine, T., Münker, C., Mezger, K., & Palme, H. 2002, Nature, 418, 952
Lee, D.-C., Halliday, A. N., Leya, I., Wieler, R., & Wiechert, U. 2002, Earth Planet. Sci. Lett., 198, 267
Leya, I., Wieler, R., & Halliday, A. N. 2003, Geochim. Cosmochim. Acta, 67, 529
Maréchal, C. N., Télouk, P., & Albarède, F. 1999, Chem. Geol., 156, 251
Markowski, A., Leya, I., Quitté, G., Ammon, K., Halliday, A. N., & Wieler, R. 2006b, Earth Planet. Sci. Lett., 250, 104
Markowski, A., Quitté, G., Halliday, A. N., & Kleine, T. 2006a, Earth Planet. Sci. Lett., 242, 1
Masarik, J. 1997, Earth Planet. Sci. Lett., 152, 181
Münker, C., Weyer, S., Scherer, E., & Mezger, K. 2001, Geochem. Geophys. Geosyst., 2, paper 2001GC000183
Nicolussi, G. K., Davis, A. M., Pellin, M. J., Lewis, R. S., Clayton, R. N., & Amari, S. 1997, Science, 277, 1281

Nicolussi, G. K., Pellin, M. J., Lewis, R. S., Davis, A. M., Amari, S., & Clayton, R. N. 1998a, Geochim. Cosmochim. Acta, 62, 1093
Nicolussi, G. K., Pellin, M. J., Lewis, R. S., Davis, A. M., Clayton, R. N., & Amari, S. 1998b, ApJ, 504, 492
———. 1998c, Phys. Rev. Lett., 81, 3583
Petaev, M. I., & Jacobsen, S. B. 2004, Meteorit. Planet. Sci., 39, 1685
Qin, L., Dauphas, N., Janney, P. E., & Wadhwa, M. 2007, Anal. Chem., 79, 3148
Quitté, G., Birck, J.-L., & Allégre, C. J. 2000, Earth Planet. Sci. Lett., 184, 83
Rauscher, T., & Thielemann, F.-K. 2000, At. Data Nucl. Data Tables, 75, 1
Savina, M. R., Davis, A. M., Tripa, C. E., Pellin, M. J., Gallino, R., Lewsi, R. S., & Amari, S. 2004, Science, 303, 649
Savina, M. R., et al. 2003, Geochim. Cosmochim. Acta, 67, 3201
Scherstén, A., Elliott, T., Hawkesworth, C., Russell, S., & Masarik, J. 2006, Earth Planet. Sci. Lett., 241, 530
Schoenberg, R., Kamber, B. S., Collerson, K. D., & Eugster, O. 2002, Geochim. Cosmochim. Acta, 66, 3151

Takahashi, K., & Yokoi, K. 1987, At. Data Nucl. Data Tables, 36, 375
Terada, K., Itoh, K., Hidaka, H., Yoshida, T., Iwamoto, N., Aoki, W., & Williams, I. S. 2006, NewA Rev., 50, 582
Trinquier, A., Birck, J.-L., & Allègre, C. J. 2007, ApJ, 655, 1179
Vockenhuber, C., Dillmann, I., Heil, M., Käppeler, F., Winckler, N., Kutschera, W., Wallner, A., & Bichler, M. 2007, Phys. Rev. C, 75, 015804
Vockenhuber, C., et al. 2004, Phys. Rev. Lett., 93, 172501
Völkening, J., Köppe, M., & Heumann, K. G. 1991, Int. J. Mass Spectrom. Ion Proc., 107, 361
Voshage, H., & Feldmann, H. 1979, Earth Planet. Sci. Lett., 45, 293
Wisshak, K., Voss, F., Käppeler, F., Kazakov, L., Becvár, F., Krticka, M., Gallino, R., & Pignatari, M. 2006, Phys. Rev. C, 73, 045807
Yin, Q.-Z., Jacobsen, S. B., Yamashita, K., Blichert-Toft, J., Télouk, P., & Albarède, F. 2002, Nature, 418, 949
Zinner, E., Amari, S., & Lewis, R. S. 1991, ApJ, 382, L47